Aqueous alteration detection in Tikhonravov crater, Mars

F. Mancarella, S. Fonti, G. Alemanno, V. Orofino, and A. Blanco[1]

[1]Dipartimento di Fisica, Università del Salento, Italy

The existence of a wet period lasting enough to allow the development of elementary forms of life on Mars has always been a very interesting issue. In this perspective, the research for geological markers of such occurrence has been continually pursued. There is considerable evidence that, during at least part of the Noachian era (from 4.1 to 3.7 Gyr ago, [1]), the Martian atmosphere, mainly composed by CO_2, was thick enough to provide a strong greenhouse effect [2–5]. The duration of these warm and wet conditions is still matter of debate, but theoretical climatic models suggest that they could have persisted for hundreds of millions up to a billion years [6–10].

It is important to note that most of the information about the surface composition of Mars and, in general, of the bodies of the Solar System has been obtained by means of reflectance spectroscopy. This technique, in fact, represents a valuable tool for remote sensing [11], being widely used in terrestrial (using field instruments, air planes or satellites), as well as in planetary researches (using ground-based telescopic observations, spacecraft or rovers missions). For the identification of rock-forming minerals, the near– and medium–infrared (NIR and MIR) regions of the electromagnetic spectrum are particularly well suited, since several diagnostic features are located in this wavelength range [12–14].

The orbital visible and near–infrared (VNIR) data from the Observatoire pour la Minéralogie, l'Eau, les Glaces, et l'Activité (OMEGA) on board of Mars Express spacecraft [15, 16] and the Compact Reconnaissance Imaging Spectrometer for Mars (CRISM) on board of Mars Reconnaissance Orbiter [17,18] have played a key role in this contest. Both instruments have revealed extensive clay bearing outcrops in regions around Nili Fossae and Mawrth Vallis [19–25], while in the southern highlands clays minerals are found in outcrops of smaller size [26,27]. But, the majority of the clay detected are associated with impact craters, in central peaks, walls or ejecta (e.g. in Jezero crater, [23], in Holden and Eberswalde craters, [28], in Gale crater, [29], and in Columbus crater, [30]).

In our work, we have focused our attention in an impact crater named Tikhonravov, located in eastern Arabia Terra (36.12°E and 13.12°N) (Figure 1*a,b*) and, in particular, in a minor crater shown in Figure 1*c*. Tikhonravov is supposed to be a paleolake [31] and therefore, the standing water may have resulted in a suitable environment for the formation of hydrated minerals.

With the aim to identify hydrated minerals, we have taken into account two CRISM footprints, one at a spatial resolution of 18 m/pixel (FRT0001175F) and one of 36 m/pixel (HRL00013C1D). These observations partially overlap as shown in Figure 1*c* and can be used to recover information about the mineralogy of the sediments visible in Figure 1*d-e*. In this perspective, we have analyzed both observation checking that the mineralogical attribution is the same. After the photometric and atmospheric correction and data filtering, we have extracted the file containing the spectral parameters for both observations. For better understanding the mineralogical distribution in these sites, we have created, for each data cube, the false colour images (RGBs) useful for the identification of water related materials, associating different color with different compositions. After that, spectra in the original CRISM cube corresponding to accumulation of pixels with the same color in the RGBs were averaged and ratioed to that of neutral region. The result was then compared to laboratory spectra extracted from the RELAB database ([32] and RELAB User's manual, http://www.planetary.brown.edu/relab/). The application of all the spectral parameters for carbonates has led to the identification, in both CRISM observations, of small deposits where carbonates could be present [33].

Carbonate-bearing deposits are identified in spectral data mainly by the presence of both ~2.3 and ~2.5 μm features, overtones of C-O stretching [34]. Since also spectra of phyllosilicates and zeolites are characterized by features located in the same positions, in order to certify the identification of carbonates, both features must be present. On the other hand

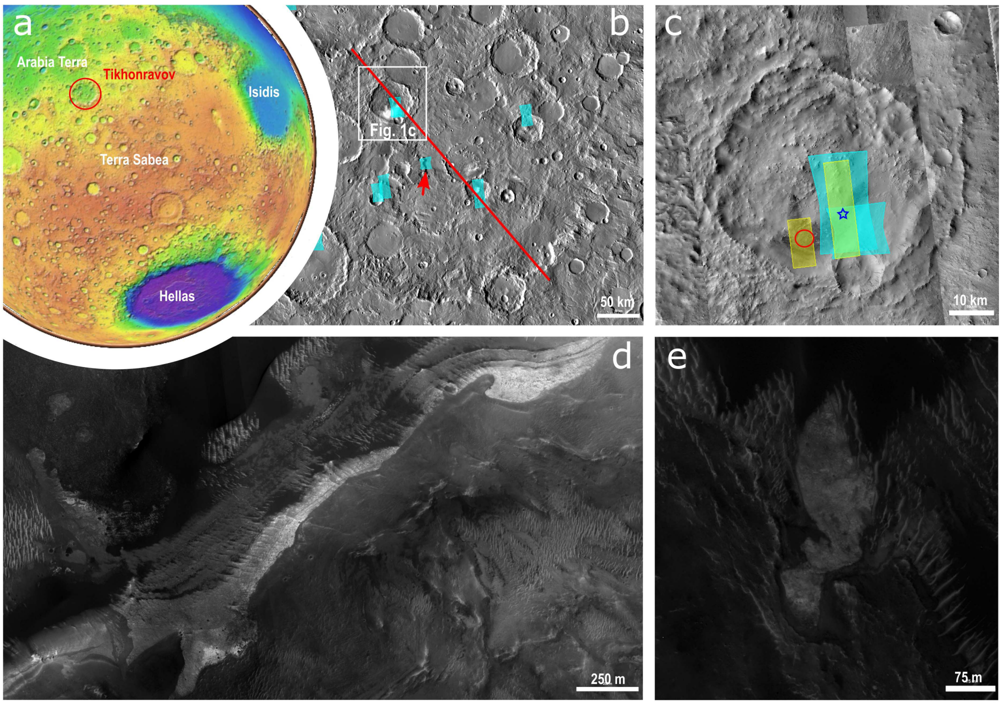

Figure 1. (**a**) MOLA colored shaded relief map of Mars showing the location of Tikhonravov impact crater (centered at 36.12°E, 13.12°N) on the southern-east part of Arabia Terra (credit: NASA/MOLA Science Team). (**b**) THEMIS IR daytime mosaic at 128 pixel/deg (credit: NASA/JPL/ASU) with superimposed CRISM observations footprints (only FRT and HRL, light blue swaths). The red line indicates the diameter of Tikhonravov crater. (**c**) Mosaic of CTX images of the studied small crater with superimposed CRISM observations footprints analyzed in this paper (FRT0001175F and HRL00013C1D, light blue swaths) and two HiRISE images acquired by the red filter of this camera (ESP_034668_1945 and ESP_013926_1945, yellow stripes). The red circle and the blue star indicate the location of Figure 1*d*-*e*, respectively. (**d**) Portion of the HiRISE image ESP_034668_1945 showing both light– and dark–toned dunes present in the analyzed region. (**e**) Magnification of ESP_013926_1945 HiRISE observation of the light-toned units that could be associated with the mineral deposits found with the analysis of CRISM observations [33].

these bands located in the spectral region 2.3-2.5 μm are weaker respect to those in the 3.0-4.0 μm range, specifically at ∼3.4 μm and ∼3.9 μm, although the strong H_2O band at 3 μm could mask them [35–39].

If we compare the average spectrum within the identified region with that of an other area spectrally unremarkable (red and black spectra in Figure 2*a* and 2*d*, respectively), we obtain the ratioed spectrum shown as a red curve in panels *b* and *e* of Figure 2. It is clear that the broad feature located at 1.9 μm and smaller ones at 1.4 and 2.29 μm (blue dashed lines in Figure 2) could be due to the presence of a phyllosilicate, probably nontronite. Together with these bands, two feature at 2.35 and 2.55 μm, indicated with dashed red lines are present in the spectra of this region in both the studied CRISM images (panels *b* and *e* in Figure 2). They could be related to the presence of some Fe-rich carbonates, such as siderite (red spectra in bottom panels of Figure 2).

Such results relative only to a minor crater of Tikhonravov, corresponding to the deepest part of the crater floor, would lead to two interpretations of the formation of the identified hydrated minerals. The first possibility is that these sediments were formed by flowing surface and then covered by various processes. In this case, the observation of hydrated deposits only in the deepest minor crater, and not in the other secondary impact structures within the main crater, can be explained by the fact that only this crater has a depth larger enough to reach the lacustrine deposits below the cover and exhume them.

Alternatively, and perhaps more probable, the fact that the hydrated minerals were not identified in all the morphological units exposing exhumed material within Tikhonravov crater, could be related to a different formation of those identified only in the minor crater. The presence of these aqueous alterations could be explained by the model that involves the existence of

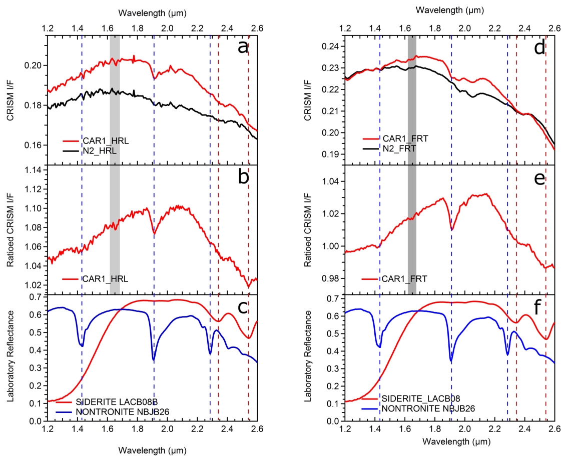

Figure 2. (**a**) Averaged spectrum from the area where carbonates were identified in HRL00013C1D. The black spectrum is the mean of spectra from chosen neutral region. (**b**) Ratioed spectrum obtained comparing the red spectrum with the black one in (*a*). (**c**) RELAB spectra of siderite (ID: LACB08, red curve) and nontronite (ID: NBJB26, blue curve). (**d**) Averaged spectra from red area where carbonates were identified in FRT0001175F. The black spectrum is the mean of spectra from chosen neutral region. (**e**) Ratioed spectrum obtained comparing the red spectrum with the black one in (*d*). (**f**) Same as in (*c*). Vertical blue dashed lines at 1.43, 1.9, and 2.29 μm indicate the central position of spectral features of nontronite, while the red ones at 2.34 and 2.55 μm those of siderite. The gray boxes in (*a*)–(*b*) and (*d*)–(*e*) indicates the presence of an instrument artifact located at 1.65 μm [33].

a hydrological activity due to groundwater circulation that occurred throughout the late Noachian and early Hesperian epochs all over Arabia Terra, the region around Tikhonravov crater.

1. Acknowledgments

Gaetano Di Achille is warmly thanked for fruitful discussions. This work has been partly supported by the Italian Space Agency (ASI), the Italian National Institute of Astrophysics (INAF) and the Italian Ministry of University and Research (MIUR). The efforts in building and developing the RELAB database are greatly acknowledged.

REFERENCES

1. Tanaka, K. L. (1986), Journal of Geophysical Research 91, E139–E158.
2. Pollack, J. B. *et al.* (1990), Journal of Geophysical Research 95, 14,595–14,627.
3. Forget, F. *et al.* (1997), Science 278, 1273–1276.
4. Yung, Y. L. *et al.* (1997), Icarus 130, 222–224.
5. Forget, F. *et al.* (2004), AGU Fall Meeting Abstracts, Abstract #P11A-0964.
6. Kleinhans, M. G (2005), Journal of Geophysical Research 110, doi:10.1029/2005JE002521.
7. Fassett, C. I., and J. W. Head (2008a), Icarus 195, 61-89.
8. Hoke, M. R., and B. M. Hynek (2009), Journal of Geophysical Research 114, doi:10.1029/2008JE003247.
9. Hynek, B. M. *et al.* (2010), Journal of Geophysical Research 115, 2156-2202.
10. Hoke, M. R. *et al.* (2011), Earth and Planetary Science Letters, 312, 1-12.
11. Hapke, B. et al. (2012), *Theory of reflectance and emittance spectroscopy*, Cambridge University Press, Cambridge.
12. Ross, H. P. *et al.* (1969), Icarus 11, 46–54.
13. Hunt, G. R., and J. W. Salisbury (1970), Mod. Geol 1, 283–300.
14. Farmer, V. C. (1974), *The infrared spectra of minerals*, Mineralogical Society, London.
15. Bibring, J.–P.*et al.* (2005), Science 307, 1576–1581.
16. Bibring, J.–P. *et al.* (2006), Science 312, 400–404.
17. Murchie, S. *et al.* (2007), Journal of Geophysical Research 112, doi:10.1029/2006JE002682.
18. Murchie, S. *et al.* (2009), Journal of Geophysical Research 114, doi: 10.1029/2009JE003342.
19. Loizeau, D. *et al.* (2007), Journal of Geophysical Research 112, doi:10.1029/2006JE002877.
20. Mustard, J. F. *et al.* (2007), Journal of Geophysical Research 112, doi:10.1029/2006JE002834.
21. Mangold, N. *et al.* (2007), Journal of Geophysical Research 112, doi:10.1029/2006JE002835.
22. Bishop J. *et al.* (2008), Science 321, 830–833.
23. Ehlmann, B. L. *et al.* (2009), Journal of Geophysical Research 114, doi:10.1029/2009JE003339.
24. McKeown, N. K. *et al.* (2009), Journal of Geophysical Research 114, doi:10.1029/2008JE003301.
25. Noe Dobrea, E. Z. *et al.* (2010), Journal of Geophysical Research 115, doi:10.1029/2009JE003351.
26. Mustard, J. F. *et al.* (2008), Nature 454, 305–309.
27. Loizeau, D. *et al.* (2012), Icarus 219, 476–497.

28. Milliken, R. E., and D. L. Bish (2010), Philosophical Magazine 90, 2293–2308.
29. Milliken, R. E. *et al.* (2010), Geophysical Research Letters 37, doi:10.1029/2009GL041870.
30. Wray, J. J. *et al.* (2011), Journal of Geophysical Research 116, doi:10.1029/2010JE003694.
31. Fassett, C. I., and J. W. Head (2008b), Icarus 198, 37–56, doi:10.1016/j.icarus.2008.06.016.
32. Pieters, C. M. (1983), Journal of Geophysical Research 88, 9534–9544.
33. Mancarella, F. *et al.* (2017), submitted.
34. Hunt, G. R., and J. W. Salisbury (1971) Mod. Geol. 2, 23–30.
35. Miyamoto, M., and A. Kato (1990), Lunar and Planetary Science Conference XXI, 801–802.
36. Cloutis, E. A. *et al.* (2000), Lunar and Planetary Science Conference XXXI, Abstract 1152.
37. Harner, P. L., and M. S. Gilmore (2015), Icarus 250, 204–214, doi:10.1016/j.icarus.2014.11.037.
38. Applin, D. M. *et al.* (2014), Lunar and Planetary Science Conference XLV, Abstract 1881.
39. Wray, J. J. *et al.* (2016), Journal of Geophysical Research 121, 652–677, doi:10.1002/2015JE004972.